Exploration of Drug Science

Open Exploration

Open Access Original Article

Cytotoxic effects of branched cationic peptides derived from bovine lactoferricin on oral squamous cell carcinoma

Diana A. Martinez-Baquero[1*], Paola A. Barato-Gomez[2], Sandra C. Vega-Chaparro[1], Jaiver E. Rosas-Perez[1]

[1]Pharmacy Department, National University of Colombia, Bogota 111321, Colombia
[2]Corpavet SAS, Bogota 111321, Colombia

***Correspondence:** Diana A. Martinez-Baquero, Pharmacy Department, National University of Colombia, Bogota 111321, Colombia. diamartinezba@unal.edu.co
Academic Editor: Fernando Albericio, University of KwaZulu-Natal, South Africa, Universidad de Barcelona, Spain
Received: March 25, 2026 **Accepted:** May 24, 2026 **Published:** July 22, 2026

Cite this article: Martinez-Baquero DA, Barato-Gomez PA, Vega-Chaparro SC, Rosas-Perez JE. Cytotoxic effects of branched cationic peptides derived from bovine lactoferricin on oral squamous cell carcinoma. Explor Drug Sci. 2026;4:1008171. https://doi.org/10.37349/eds.2026.1008171

Abstract

Aim: Squamous cell carcinoma (SCC) is one of the most common types of cancer affecting the oral cavity and the upper aerodigestive tract. In many cases, misdiagnosis leads to the progression of the disease to life-threatening stages, highlighting the importance of advancing anti-oral cancer therapeutics. In this study, we evaluated the cytotoxic activity against SCC of a series of synthetic peptides derived from bovine lactoferricin (bLFcin). To enhance the cationic and amphiphilic properties of lactoferricin-derived peptides, we designed branched and palindromic sequences from bLFcin(20-25) (i.e., 20RRWQWR25).

Methods: A total of 14 peptides were synthesized using solid support synthesis. More than 90% peptide purity was obtained by solid-phase extraction, and the final products were characterized using reversed-phase liquid chromatography and mass spectrometry. The in vitro cytotoxic activity of the peptides was assessed in cancer cell lines SCC9 and FaDu; HEK001 keratinocytes were used as a non-cancerous control cell line. Additionally, scanning electron microscopy and flow cytometry provided further insights into the peptide-cell interaction. Finally, the dimeric peptide bLFcin$(20\text{-}25)_2$ was evaluated in a chemically-induced carcinoma in vivo model.

Results: Tetrameric and dimeric peptides with higher cationic charge and improved amphiphilic properties were cytotoxic to the oral carcinoma cell line FaDu. Scanning electron microscopy revealed membrane disruption and pore formation. In addition, flow cytometric analyses of cells treated with fluorescently tagged bLFcin$(20\text{-}25)_2$ confirmed the interaction of the cationic peptide with the anionic cancer cells. Furthermore, the dimeric peptide bLFcin$(20\text{-}25)_2$ inhibited tumor growth of chemically induced oral carcinoma in hamsters, demonstrating its in vivo efficacy.

Conclusions: Branched peptides with a higher cationic charge were cytotoxic to the cancer cell line FaDu; they induced cell membrane lysis, as evidenced by electron microscopy, and inhibited tumor progression in hamsters. These preliminary results support further design and mechanistic evaluation of branched cationic peptides as potential oral cancer therapeutics.

Keywords

antimicrobial cationic peptides, lactoferricin, oral squamous cell carcinoma, solid-phase peptide synthesis

Introduction

Squamous cell carcinoma (SCC) is the most common type of cancer in the upper aerodigestive tract, accounting for over 90% of malignancies in the mouth and oropharynx [1]. In many low-income countries, diagnoses occur at advanced stages due to limited access to adequate healthcare. The 5-year overall survival rate in these countries (35–37%) is significantly lower than in other more developed nations (~50%) [2]. Once cancer develops, it is vital to determine the extent, location, and histological features of the lesion. The most common treatment involves resection of the affected area, followed by chemoradiotherapy. Unfortunately, adverse effects are common and negatively impact patients' quality of life [3]. Recently developed targeted therapies aim to reduce the side effects of cytotoxic agents, and combining these approaches with chemoradiotherapy has the potential to improve treatment outcomes for patients with locally advanced SCC of the head and neck compared to chemoradiotherapy alone [4]. Electrochemotherapy has also emerged as a promising alternative. By combining electroporation with cytotoxic agents such as bleomycin, this method has been shown to increase survival rates for patients with early-stage oropharyngeal cancer [5]. Furthermore, adopting multimodal treatment plans that include targeted and adjuvant therapies could significantly benefit patient prognosis. In this regard, cationic antimicrobial peptides (CAMPs) have been extensively studied as anticancer treatments [6–11]. The chemical and physicochemical versatility of these host defense peptides enables modifications, such as the conjugation of CAMPs to antimetastatic antibodies [12], and the organelle-targeting of chemically modified cationic peptides [13, 14] and fatty acid derivatives [15].

Lactoferrin (Lf) is a nonheme iron-binding glycoprotein secreted by epithelial cells of the mammalian mucosa and is especially abundant in human colostrum (6–8 mg/mL) and breast milk (2–4 mg/mL). These high levels, which exceed those found in other body fluids and in the milk of other mammals, play a key role in regulating iron absorption and protecting newborns from gastrointestinal infections. Bovine lactoferricin (bLFcin), a CAMP derived from the N-terminal lobe of bovine Lf (bLf) through pepsin hydrolysis, is a 25-residue peptide that adopts an antiparallel β-sheet structure, stabilized by an intramolecular disulfide bond, and exhibits potent antimicrobial activity. This activity is associated with its highly basic nature, enriched in positively charged arginine and lysine residues, as well as the presence of tryptophan residues that are critical for function [16]. These features enable electrostatic interactions between lactoferricin or other cationic peptides and negatively charged molecules expressed on cancer cell membranes (e.g., phosphatidylserine). This property confers cationic peptides with specificity against tumor cells [17–20]. Indeed, lactoferricin and its derived peptides have been shown to have cytotoxic activity against various cancers (e.g., lung, ovarian, squamous cell, colon) and hematological malignancies [21–30].

We have demonstrated that a 6-amino acid motif (i.e., RRWQWR) is essential for antimicrobial [30, 31] and cytotoxic activity [32]. Notably, a tetrameric branched peptide with the motif RRWQWR repeated four times displayed enhanced chemotherapeutic activity in in vivo models of infection and oral SCC (OSCC). In the latter, we demonstrated that the intratumoral administration of a tetrameric branched construct, containing four copies of the cationic motif RRWQWR, effectively inhibited the growth of oral tumors in hamster buccal pouches. However, evidence of necrotic activity and dense lymphocytic infiltration raised concerns regarding the safety of this cytotoxic peptide [33]. Furthermore, subsequent evaluations of the tetrameric bLFcin(20-25)$_4$ revealed significant toxicity, with hemolytic activity exceeding 50% in human erythrocytes [34]. To better understand the cytotoxic activity and the functional role of individual amino acids within the linear sequence bLFcin(17-31), the natural precursor containing the RRWQWR motif, we conducted a structure-function analysis. Specifically, we assessed the cytotoxicity of linear peptides truncated at the carboxyl and amino termini using human SCC9 and FaDu hypopharyngeal SCC cell lines, with healthy keratinocytes HEK001 serving as controls. Additionally, we evaluated branched arrangements

of the repeated RRWQWR motif, including a palindromic sequence with an increased cationic charge and a dimeric construct; these cationic peptides were compared against their tetrameric counterpart. Our in vitro screening identified a branched peptide with modest cytotoxic activity in hypopharyngeal SCC, which was subsequently tested for anti-tumorigenic properties in vivo using a chemically induced animal model of OSCC [35].

Materials and methods

Materials and reagents

Rink amide resin, 9-fluorenylmethoxycarbonyl (Fmoc) amino acids, 6-HCl 1-hydroxybenzotriazole (HOBt), and *N*,*N*-dicyclohexylcarbodiimide (DCC) were purchased from AAPPTec (Louisville, KY, USA). Methanol, diethyl ether, *N*,*N*-dimethylformamide (DMF), absolute ethanol, dichloromethane (DCM), acetonitrile (ACN), isopropyl alcohol (IPA), trifluoroacetic acid (TFA), ethane-1,2-dithiol (EDT), and triisopropylsilane (TIS) were obtained from Merck KGaA (Darmstadt, Germany). 4-methylpiperidine, pyridine, Triton-X, potassium cyanide (KCN), phenol, ninhydrin, biotin-NHS, Supelclean LC-18 SPE columns, α-cyano-4-hydroxycinnamic acid, ethylenediaminetetraacetic acid (EDTA), Trypan blue, hydrocortisone, doxorubicin hydrochloride, resazurin sodium salt, 7,12-dimethylbenz[α]anthracene (DMBA), dexamethasone sodium phosphate and trypsin were obtained from Millipore-Sigma (St. Louis, MO, USA).

Peptide synthesis and characterization

All bLFcin-derived peptides (Table 1) were manually synthesized by solid-phase peptide synthesis (SPPS) using a previously described Fmoc/tert-butyl (tBu) protection strategy [36]. Briefly, (a) Rink amide resin (0.46 meq/g) was swollen in DMF for 15 min with constant stirring and washed 3 times with DCM. (b) Fmoc removal reactions were carried out using 25% 4-methylpiperidine (Triton-X 1%) in DMF for 10 min at room temperature; this treatment was repeated once, and the resin was then washed 5 times with DMF and 3 times with DCM. (c) We performed the Kaiser test to verify free amine groups on the resin during subsequent Fmoc deprotection steps along the synthesis. (d) For the coupling reaction, 5 eq of each Fmoc-protected amino acid, 5 eq of DCC, and 5 eq of HOBt were dissolved in DMF and added to the resin with constant stirring for a minimum of 3 h. The coupling reaction was monitored with the Kaiser test until a negative result was obtained. (e) Cleavage of the full amino acid sequence and the deprotection of the sidechain protecting groups were carried out by adding a cleavage cocktail solution of TFA/water/TIS/EDT (92.5/2.5/2.5/2.5, v/v) for 3 h with constant stirring at room temperature (20–23°C). The solution from the resin and cleavage cocktail mixture was recovered by filtration, and the peptide was precipitated using 2 volumes of ice-cold diethyl ether. The dried pellet was resuspended in water for lyophilization; 500 µL of the solution was reserved for high-performance liquid chromatography (HPLC) and characterization. (f) Crude peptides were purified by reversed-phase solid-phase extraction using Supelclean C18 silica columns (5 g LC-18 SPE). After activating the column according to the manufacturer's instructions, the crude peptide (50 mg/mL) was loaded onto the column, and a stepwise gradient from 0% to 90% ACN in water was applied to purify the peptide. The fractions were pooled based on their HPLC-analyzed purity (> 90%), and lyophilized. Peptide purity was determined by HPLC by injecting 10 µL of peptide solution (1 mg/mL) and eluting using a linear 2 mL/min, 10 min, 5% to 70% gradient of ACN 0.05% TFA in water 0.05% TFA, in an Agilent 1200 LC system equipped with a Chromolith C18 column (50 mm × 4.6 mm) and a UV detector set at 210 nm.

Molecular weights were confirmed by matrix-assisted laser desorption/ionization–time of flight (MALDI–TOF): MALDI–TOF mass spectrometry using an Ultraflex III TOF/TOF mass spectrometer (Bruker Daltonics, Bremen, Germany) operated in reflector mode, with an MTP 384 polished steel target plate (Bruker Daltonics) and α-cyano-4-hydroxycinnamic acid as the matrix. Spectra were acquired using 500 laser shots at 25–30% laser power.

The synthesis of the dimeric branched peptide bLFcin(20-25)$_2$ involved the double elongation of the L-lysine chain at both the N-alpha and N-epsilon termini. The tetrameric branched peptide bLFcin(20-25)$_4$ was produced through dimerization, which utilized oxidative disulfide bridging of the C-terminal Cys

Table 1. Synthetic peptides derived from bLFcin.

Peptide group	Amino acid sequence	Code	Net charge (pH 7.0)	MS MALDI–TOF	
				Exact mass	*m/z*
bLFcin	FKC**RRWQWR**MKKLGA	bLFcin(17-31)	6	1,993.5	1,994.71
	FKC**RRWQWR**MKKLG	bLFcin(17-30)	6	1,922.4	1,922.48
	FKC**RRWQWR**MKKL	bLFcin(17-29)	6	1,865.3	1,865.73
C-terminus truncated	FKC**RRWQWR**MKK	bLFcin(17-28)	6	1,752.2	1,752.55
	FKC**RRWQWR**MK	bLFcin(17-27)	5	1,624.0	1,625.19
	FKC**RRWQWR**M	bLFcin(17-26)	4	1,495.8	1,497.06
	FKC**RRWQWR**	bLFcin(17-25)	4	1,364.6	1,365.82
N-terminus truncated	KC**RRWQWR**MKKLGA	bLFcin(18-31)	6	1,846.3	1,849.12
	C**RRWQWR**MKKLGA	bLFcin(19-31)	5	1,718.1	1,718.01
	RRWQWRMKKLGA	bLFcin(20-31)	5	1,615.0	1,617.38
	RRWQWR	bLFcin(20-25)	3	986.1	986.66
Polyvalent forms	**(RRWQWR)**$_2$KAhx	bLFcin(20-25)$_2$	6	2,196.2	2,198.51
	[**(RRWQWR)**$_2$KAhxC]$_2$	bLFcin(20-25)$_4$	12	4,597.5	2,302.96*
	RWQWRWQWR	bLFcinPal	3	1,486.7	1,488.58

The 6-amino-acid motif with reported antibacterial activity is shown in bold. Net charge was calculated by adding the net charges of basic/acidic residues at pH 7.0. *m/z*: for monoisotopic masses $[M + H]^+$. * The *m/z* of the peptide was confirmed in its monomeric form prior to oxidative dimerization. MALDI–TOF: matrix-assisted laser desorption/ionization–time of flight.

monomer in a solution of phosphate buffer (pH 8.0) and 10% DMSO (see Figure 1). HPLC was used to monitor the conversion of the dimer to the tetramer until the reaction was complete.

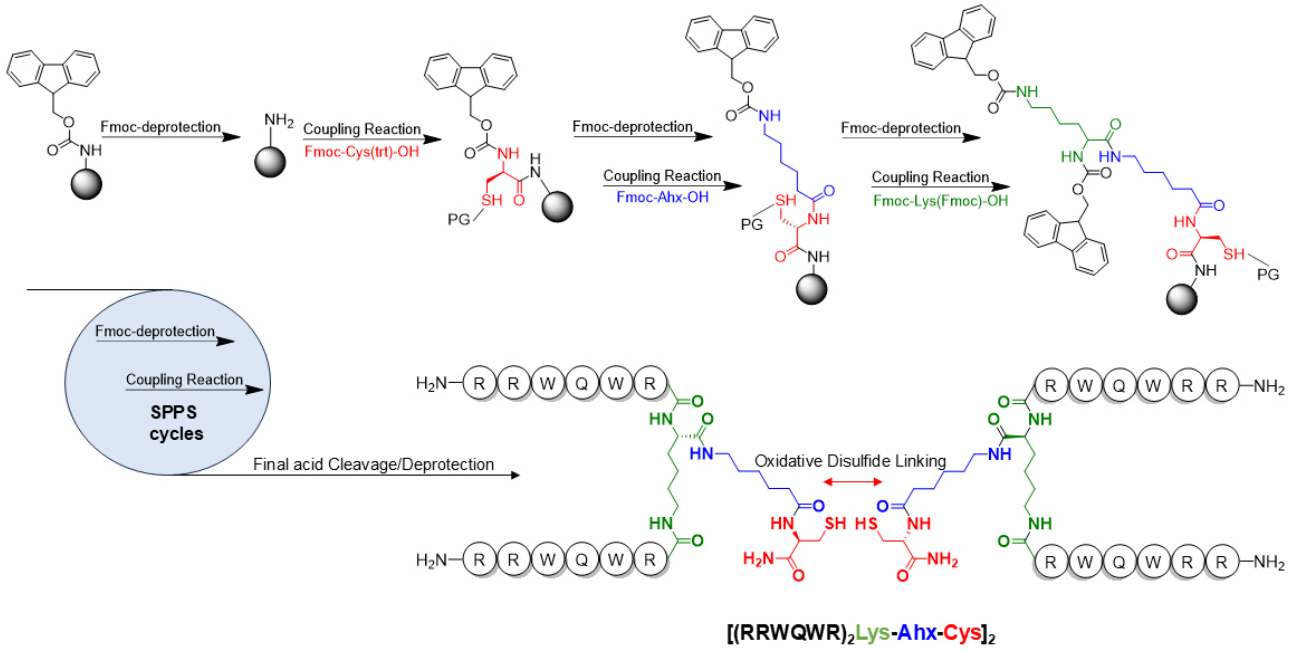

Figure 1. Synthesis of bLFcin(20-25)$_4$ via solid-phase peptide synthesis and oxidative disulfide linking.

Peptides (purity > 90%) were dissolved in sterile phosphate buffered saline (PBS) to achieve final concentrations ranging from 100 to 6.25 μM (for most peptides) or from 50 to 3.125 μM (for the tetrameric peptide). For in vivo assays, the dimeric peptide was dissolved to 100 μM in sterile saline.

Cell culture

The human OSCC cell lines FaDu (ATCC® HTB-43™) and SCC9 (ATCC® CRL-1629™), and the human keratinocyte line HEK001 (ATCC® CRL-2404™) were purchased from the American Type Culture Collection (ATCC-Manassas, VA). Cell culture was performed strictly following the ATCC recommendations, and only

one cell line was manipulated at a time to avoid cross-contamination. FaDu cells were cultured in RPMI medium (L0500, Biowest) supplemented with 10% fetal bovine serum (S1810, Biowest). SCC9 cells were cultured in DMEM/F12 medium (L0093, Biowest) supplemented with 400 ng/mL hydrocortisone and 10% FBS. HEK001 keratinocytes were cultured in serum-free KGM BulletKit medium containing the supplements included in Lonza Corporation®'s kit CC 3107. All cells were maintained in a 5% CO_2 humidified atmosphere at 37°C. The culture media were changed every 2–3 days; cells were passaged twice a week and used between 6 and 10 generations. Trypan blue dye was used routinely to quantify cell viability and density. Mycoplasma infection was assessed when thawing a new vial from each cell master bank using the Mycoplasma Detection Kit MycoStrip® (Invitrogen).

Assessment of peptide-induced cytotoxicity

The cytotoxic activity of all peptides was evaluated using the resazurin assay, which measures cell viability. Cells were plated onto 96-well tissue culture plates (FaDu = 1.2×10^4 cells/well; SCC9 = 1.0×10^4 cells/well; and HEK001 = 1.4×10^4 cells/well) and allowed to attach for 18 h until they reached 70–80% confluence. We then incubated the cells with 100, 50, 25, 12.5, and 6.25 µM bLFcin-derived peptides; the tetrameric peptide bLFcin(20-25)$_4$ was tested at 50, 25, 12.5, 6.25, and 3.125 µM. Doxorubicin (10 µM) was used as a positive control for cytotoxicity; 100% cell viability was established after the addition of PBS (10 µL) to untreated control cells. Cell micrographs were obtained using phase contrast microscopy (DMi1, Leica-microsystems). After treatment for 2, 6, and 24 h, cells were rinsed with PBS, and 10 µL of resazurin 440 µM with 90 µL of medium was added to reach a final concentration of 44 µM. Metabolically active cells converted resazurin (blue-purple) to resofurin (pink); fluorescence was measured at excitation and emission wavelengths of 535 nm and 595 nm, respectively (TECAN® Genios). The fluorescence intensity of the treated cells was normalized to establish the percentage of viable cells relative to untreated counterparts. The half-maximal inhibitory concentration (IC_{50}) was calculated by plotting cell viability versus the log of peptide concentration (µM) and analyzed (GraphPad Prism 10 software) using a nonlinear regression (sigmoidal curve) fit.

Flow cytometry-based determination of cell-peptide interactions

Cells were treated with biotin-labeled bLFcin(20-25)$_2$ to evaluate its ability to permeate through the cell membrane. FaDu and HEK001 cell suspensions (2×10^5 cells/mL) were treated with 100 µM biotin-labeled bLFcin(20-25)$_2$ for 2 h. Negative control cells were treated with PBS, and peptide control cells were treated with 100 µM biotin-bLFcin(20-25), the linear 6-residue peptide. Each cell suspension (100 µL) was seeded onto 96-well, rounded-bottom plates. The plates were then centrifuged (700 *g* × 3 min), the cells rinsed with PBS, and stained with 1:1,600 phycoerythrin (PE)-streptavidin conjugate (189737, Sigma-Aldrich) in PBS. After incubation for 30 min at 4°C in the dark, excess PE-streptavidin was removed by centrifugation, and the plates were washed with PBS. Cellular PE fluorescence was measured using a flow cytometer (BD FACSCanto II). We acquired a total of 10,000 events per sample. The abundance distribution of PE-streptavidin-stained cells was determined using the FACSDiva v7.0 software.

Scanning electron microscopy (SEM)

bLFcin(20-25)$_2$-treated and untreated FaDu cells were fixed on glass coverslips using 3% glutaraldehyde in PBS (pH 7.0) for 2 h, rinsed with deionized and 0.22 µm-filtered water, and fixed in 0.5% osmium tetroxide for 45 min. We then performed 3 additional 10-min washes with filtered, deionized water and dehydrated the samples using increasing ethanol concentrations: 2× 70%, 2× 95%, and 3× 100%. Coverslips were maintained in 100% ethanol until dry, then flushed with CO_2 at critical-point conditions using a SAMDRI®-795 instrument and subsequently covered with gold nanoparticles in a Denton Vacuum Desk IV thin-film deposition system. SEM images were acquired using a JEOL JSM 6490-LV microscope.

Animals, oral carcinogenesis model, and peptide treatment

Six-week-old male Syrian golden hamsters (*Mesocricetus auratus*) were procured from the National Institute of Health of Colombia (Bogotá, Colombia). We housed 2 animals per cage in individually ventilated

filter-capped polypropylene cages (RAIR OneCage® system) at a controlled temperature (20–24°C), with a 12-h dark/light cycle; drinking water and a dry food (LabDiet 5010) were provided *ad libitum*. All animal experiments complied with the ARRIVE guidelines and the Guide for the Care and Use of Laboratory Animals. They were carried out following the EU directive 2010/63 for the protection of animals used for scientific purposes, and were approved by the Ethics Committee of the Sciences Faculty of the National University of Colombia (approved main project identification: RC# 678 of 2014).

The hamsters' right pouches were painted with a 0.5% DMBA oil solution 3 times a week for 12–16 weeks. Immunosuppression was achieved by administering daily subcutaneous dexamethasone (1 mg/kg) for 7 days, and repeated every 3 weeks during the carcinoma induction period [35]. Peptides were administered intratumorally once macroscopic lesions were evident. Animals that developed oral carcinoma were divided into 2 groups: Group A (control): 5 animals were treated daily with saline (50 µL) for 15 days; and Group B: 5 animals were treated with bLFcin(20-25)$_2$ (50 µL, 100 µM) daily for 15 days.

Tumor volume determination, euthanasia, and microscopic analyses

Once macroscopic lesions were detected, tumor dimensions (length and width) were measured daily for 15 consecutive days with a digital caliper. The tumor volume was calculated using the formula V = 0.52 × length × width^2 [37]. After 15 days of treatment, the hamsters were euthanized by intraperitoneal injection of 300 µL Euthanex® (390 mg/mL sodium pentobarbital and 50 mg/mL sodium diphenylhydantoin), and buccal pouches were procured for standard histological analyses. Tumors were fixed in buffered 3.7% formaldehyde solution, processed for routine H&E staining, and evaluated by light microscopy using an Olympus CX21 microscope.

Statistical analysis

Cytotoxic assays were conducted in cell lines in triplicate (n = 3). The IC_{50} values were ascertained via non-linear sigmoidal fit regression and are expressed as the mean ± standard error of the mean (s.e.m.). To assess the in vivo anticancer efficacy of bLFcin(20-25)$_2$, the tumor volume growth ratio was plotted against the duration of treatment (days). Statistical comparisons between the distinct groups were conducted using One-way ANOVA and Tukey's test. A *p-value* of < 0.05 was considered statistically different. All statistical analyses were carried out using GraphPad Prism version 10.

Results

Peptide synthesis and characterization

bLFcin(17-31) is a linear peptide with demonstrated antibacterial activity; however, shorter sequences obtained by depleting the amino acids at the carboxyl-terminus and conserving the amino-terminus unaltered, e.g., bLFcin(17-26), still show potent cytotoxic activity [38]. More recently, it has been studied how not only the length of immune peptides influences their bioactivity, but also how their shape and configuration play a critical role. Molecular dynamics simulations revealed that greater antibacterial activity of multiple antigenic peptides, here referred to as 'branched', results from stronger adsorption to and interaction with bacterial membranes, causing greater membrane deformation compared to linear peptides [39]. For this reason, peptides derived from bLFcin(17-31) were generated by SPPS using an orthogonal Fmoc/tBu protection strategy, as previously described [36, 40] and detailed in the Materials and methods section. The tetrameric peptide was obtained by oxidative disulfide bonding in solution of two dimeric monomers, and it is illustrated in Figure 1. Purification via solid-phase extraction and subsequent characterization resulted in peptides with purity greater than 90%, and their masses were confirmed by MALDI–TOF analyses. A complete list with the corresponding HPLC chromatograms and *m/z* mass spectrograms is available in the supplementary material (Table S1). Table 1 presents the sequences of the synthetic bLFcin-derived peptides obtained for this study; please note that all synthetic peptides are C-terminal amides.

Branched peptides exhibit greater cytotoxic activity

We next compared the ability of the peptides listed in the 3 groups shown in Table 1 to induce cytotoxicity in oral cancer cells compared to normal keratinocytes, HEK001. Our results are systematically presented below.

bLFcin peptides with truncated C-termini

These peptides harbored an intact N-terminal end and progressively shortened C-terminus. Most peptides in this group exhibited similar cytotoxic activity. Specifically, the longest representative peptide, bLFcin(17-30), showed mild cytotoxicity toward FaDu cells, decreasing cell viability to 83%; however, this effect was not significantly different from that of the other peptides in this group. Similarly, bLFcin(17-30) 100 μM decreased the cell viability of non-cancerous HEK001 cells to 68%, with sustained activity after 6 h. The decrease in viability of healthy cells suggests that bLFcin(17-30) may have deleterious effects; for this reason, further evaluation of this candidate was not pursued. In contrast, SCC9 cells were completely resistant to treatment with these peptides, even after 24 h. These findings suggest that C-terminal truncation may influence the cytotoxic activity of the full-length reference peptide bLFcin(17-31). The shortest motif from the C-terminal truncated group was found to be bLFcin(17-30) with moderate cytotoxic activity; however, cell viability of healthy HEK001 was adversely affected (see Figure S1, part A).

bLFcin peptides with N-termini truncated

N-terminal changes impacted the cytotoxic activity of the series bLFcin(18-31) to bLFcin(20-31). We observed nearly 100% viability in both tumorigenic and normal cells exposed to this peptide group (even at the highest concentration and longest incubation time—100 μM for 24 h, Figure S1, part B), indicating that the N-terminus Phe17 could play a critical role in the activity of the linear bLFcin(17-31).

Polyvalent and branched peptides derived from the RRWQWR motif

We first observed that the 6-amino-acid sequence reported as the minimal unit inducing cytotoxic and antibacterial activity did not affect cell viability (Figure 2). In contrast, polyvalent structures derived from this motif induced cytotoxicity to varying degrees. First, the tetrameric peptide bLFcin(20-25)$_4$, tested at lower concentrations, reduced the viability of the three cell lines to below 1% at the highest concentration (50 μM; Figure 2). This peptide did not preferentially target cancer cell lines, as it demonstrated similar cytotoxicity toward keratinocytes (HEK001). Its IC_{50} for FaDu, HEK001, and SCC9 cells were 7.30 ± 0.26 μM, 12.06 ± 0.68 μM, and 34.90 ± 1.18 μM, respectively (Table 2).

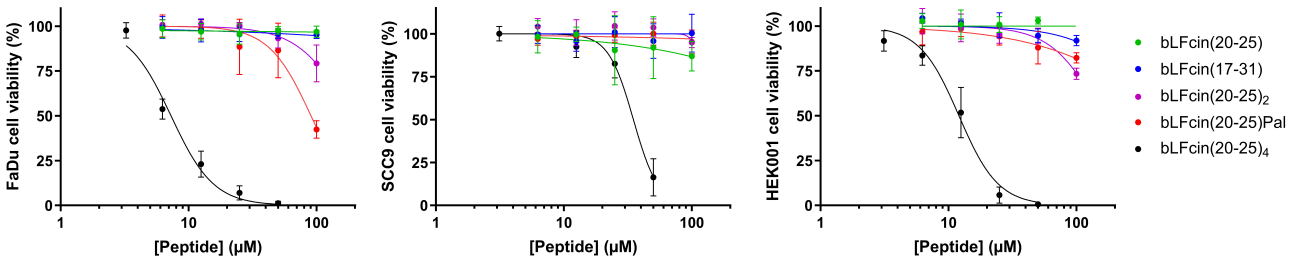

Figure 2. Cell viability following a 2-h treatment of FaDu, SCC9, and HEK001 ATCC cell lines with various concentrations (μM) of the indicated peptides.

Second, the dimeric peptide bLFcin(20-25)$_2$ was found to be a polyvalent and branched alternative to the tetrameric peptide. Its IC_{50} value for cancer FaDu cells was 185.3 ± 34.8 μM and 157.9 ± 26.9 μM for normal keratinocytes HEK001, exhibiting moderate cytotoxic activity, with no statistically significant difference when compared to its linear counterpart bLFcin(20-25); SCC9 viability remained largely unaffected, with an IC_{50} above 200 μM (Table 2). Lastly, the palindromic peptide bLFcinPal exhibited cytotoxicity only against cancer FaDu cells (IC_{50} = 90.5 ± 7.4 μM), statistically different from the linear bLFcin(20-25) (Dunnet's $p < 0.05$) (Figure 2). In contrast to the dimeric and palindromic peptides, to which

Table 2. IC_{50} (μM) calculated from sigmoidal fits of cell viability percentage vs. log (peptide concentration) plots.

Peptide	IC_{50} (μM)		
	FaDu	SCC9	HEK001
bLFcin(17-31)	> 200	> 200	> 200
bLFcin(20-25)	> 200	> 200	> 200
bLFcinPal	90.5 ± 7.4*	> 200	> 200
bLFcin$(20-25)_2$	185.3 ± 34.8	> 200	157.9 ± 26.9
bLFcin$(20-25)_4$	7.3 ± 0.26*	34.9 ± 1.18*	12.06 ± 0.68*

* Statistically significant differences against bLFcin(20-25) IC_{50}, Dunnet tested ($p < 0.05$).

keratinocytes and SCC9 cells were more resistant, the tetrameric peptide was strongly cytotoxic even at lower concentrations.

bLFcin$(20-25)_2$-induced cell morphological changes

The strong cytotoxic effect of the tetrameric peptide on normal keratinocytes raised concerns about pursuing further experimentation with this candidate, particularly given its reported hemolytic activity (H_{max} = 49.1% of red blood cells at 100 μM and 37°C) [41]. In contrast, the dimeric peptide exhibits a much lower hemolytic index (H_{max} = 5.6%) and has been reported to display cytotoxic activity against multiple cancer cell lines, including colon, breast, cervix, and prostate [42], making it a more promising candidate for further evaluation against oral cancer cell lines. Although the palindromic peptide showed higher cytotoxicity toward FaDu cells, it has also been reported to be hemolytic (H_{max} = 24.8%). Despite a higher IC_{50} of the tetramer and palindromic peptides, the modest cytotoxicity of bLFcin$(20-25)_2$ toward FaDu cells prompted its selection as a branched peptide model. The dimeric peptide bLFcin$(20-25)_2$ comprises 2 copies of the RRWQWR minimal sequence linked to a lysine by its α-amino and ε-amino termini. The cytotoxicity of the two-branched peptide was evaluated microscopically in FaDu cells (Figure 3, left panel); we observed cell membrane lysis, loss of adhesion, and expulsion of intracellular content after a 2-h treatment (100 μM). After 6 h and 24 h, the irreversible damage caused to the integrity of FaDu cells prevented their recovery. In contrast, although HEK001 keratinocytes exhibited morphological changes after 6 h of bLFcin$(20-25)_2$ exposure (Figure 3, right panel, second row), including apparent detachment and membrane blebbing, they recovered after 24 h. Lastly, SCC9 cells were highly resistant to the dimeric peptide (Figure 3, middle panel). The SCC9 cell line is reported to be significantly more chemo-resistant than similar SCC lines, such as SCC4 or SCC15 [43]. While miRNA expression and its downstream pathways contribute to these resistance mechanisms, evaluating the molecular pathways specifically related to bLFcin-derived peptides is beyond the scope of this study.

Cationic bLFcin$(20-25)_2$ interacts with FaDu and HEK001 cells and promotes internal structural changes

We next compared the ability of biotin-conjugated linear bLFcin(20-25) and dimeric bLFcin$(20-25)_2$ to elicit morphological changes and interact with FaDu and HEK001 cells using flow cytometry (FC) (Figure 4). We exposed these cells to each biotinylated peptide for 2 h, then stained them with a streptavidin-PE (SAPE) conjugate, rinsed them, and analyzed them by FC. Morphological alterations (granularity) were assessed by changes in the side-scatter signal (SSC-A [side scatter (for sample A)] vs. FSC-A [forward scatter (for sample A)], Figure 4). We found that treatment with bLFcin$(20-25)_2$ (bottom panel) increased SSC-A values, whereas the short linear motif bLFcin(20-25) (middle panel) maintained SSC-A values similar to those of untreated cells (top panel). These observations suggest that the dimeric peptide promotes internal structural changes.

We complemented our morphological analyses with fluorescence-based quantification using the "count vs. PE-A" histogram. After treatment of the cells with the dimeric peptide, the morphological alterations and potential poration of the cell membrane caused an internalization of the biotin-peptide; these cells were not permeabilized prior to the SAPE conjugate tagging, indicating that the fluorescent population had

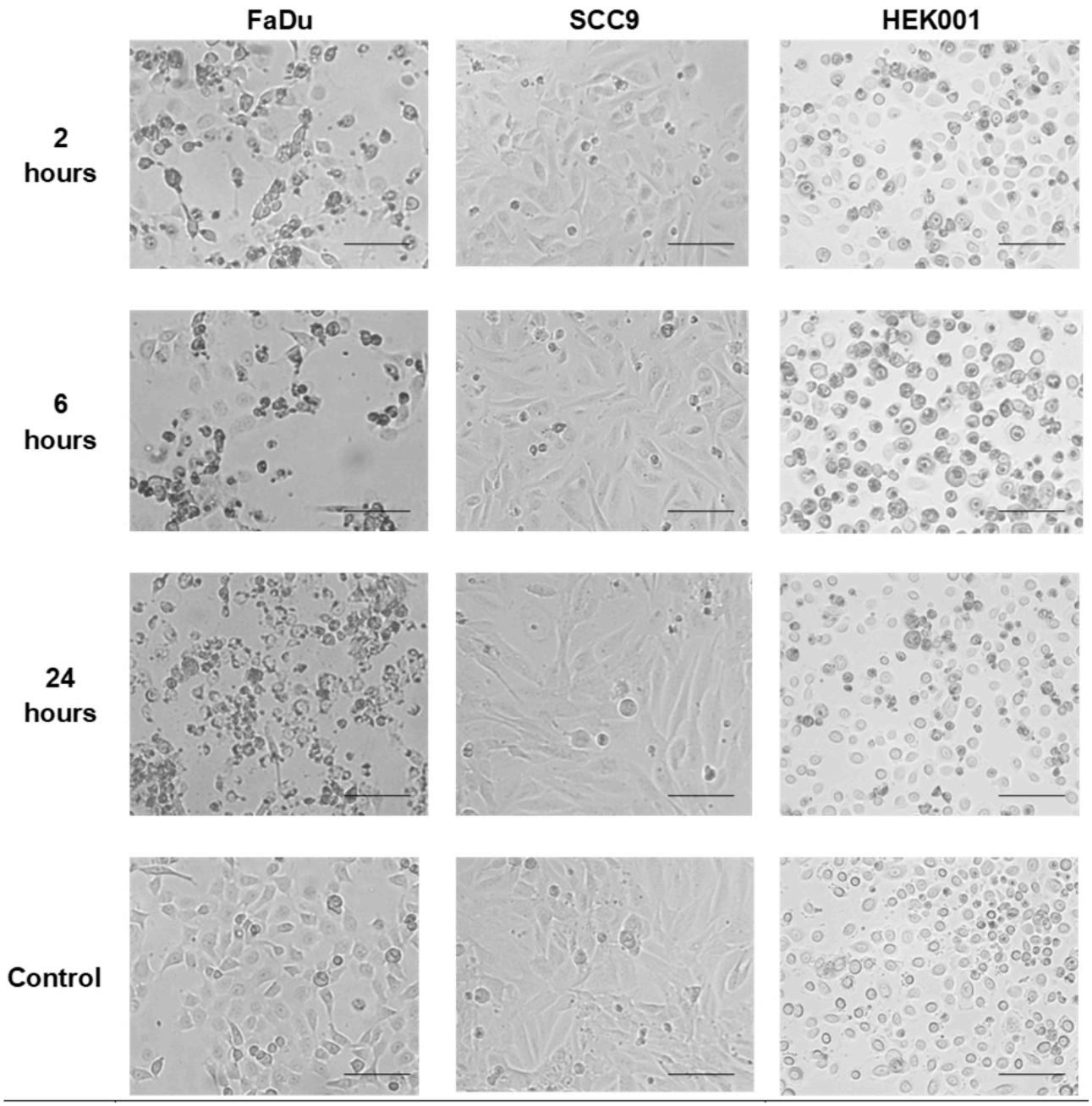

Figure 3. Photomicrographs of FaDu, SCC9, and HEK001 cells following treatment with 100 μM bLFcin(20-25)$_2$ for 2, 6, and 24 h. Scale bar = 100 μM. Control: untreated cells.

interacted and retained the biotinylated substrate, the peptide, even after the washes subsequent to the fluorescent labeling. Cells that internalized the biotin-peptide were tagged with the SAPE conjugate, enabling detection via FC due to the fluorescence properties of PE. We found that 98.4% of FaDu cells and 96.9% of HEK001 cells retained the biotinylated peptide within their structure (Figure 4, bottom panels). In contrast, untreated cells or those treated with the linear peptide RRWQWR (Figure 4, top and central panels) displayed minimal fluorescence, indicating limited peptide-cell interaction. In summary, our FC analyses confirmed dimeric peptide interaction and demonstrated its ability to induce morphological changes. However, further studies are needed to evaluate the peptide's intracellular uptake by healthy HEK001 cells and its implication in selective cytotoxicity.

bLFcin(20-25)$_2$ induces cell membrane alterations

We next investigated the effects of the dimeric peptide bLFcin(20-25)$_2$ on the cell membrane of carcinogenic FaDu cells using SEM. Following a 2-h treatment, we observed cell membrane alterations,

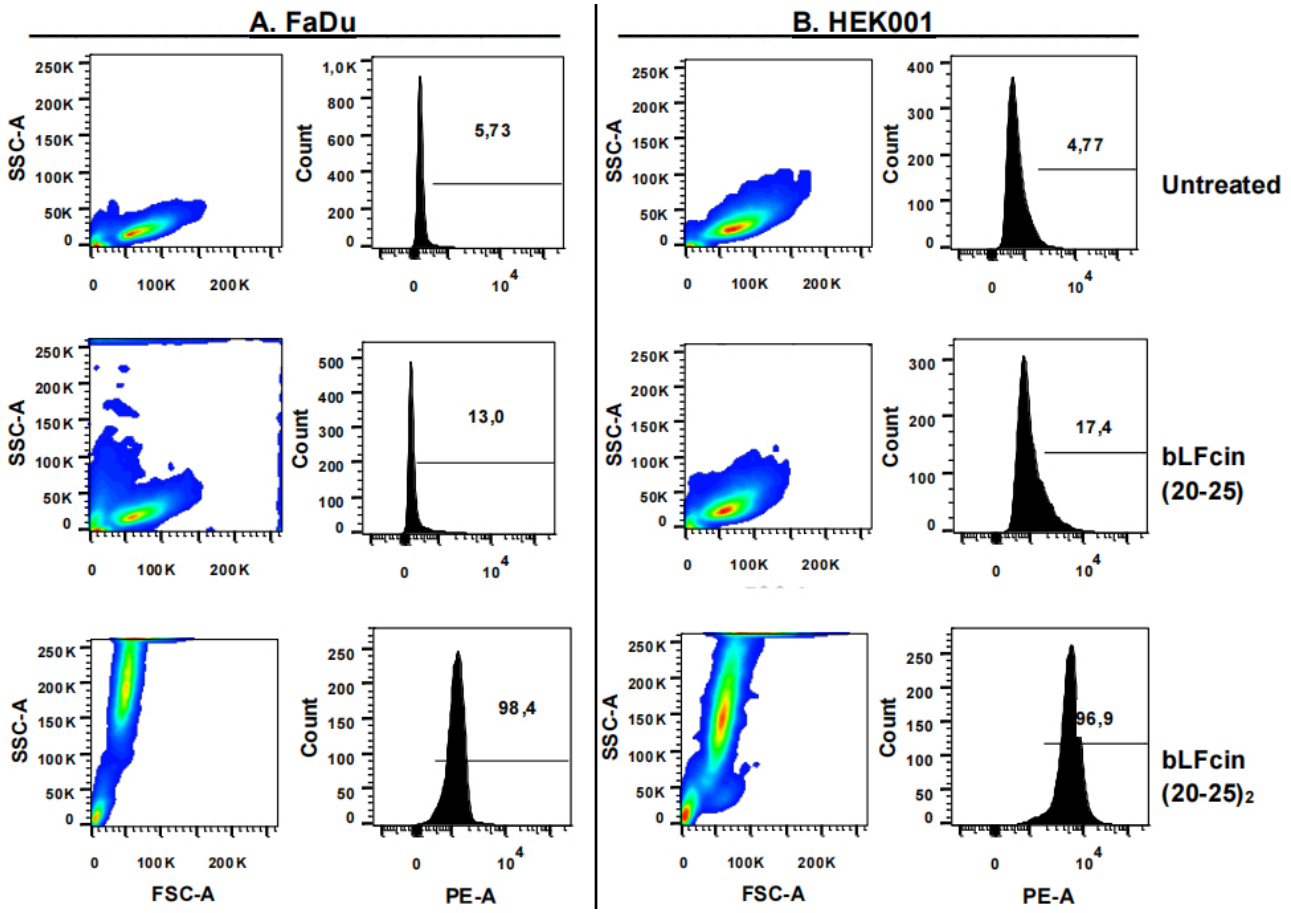

Figure 4. Flow cytometry analysis of biotinylated peptides interacting with the carcinogenic cell line FaDu and normal keratinocytes HEK001. The PE-A-augmented signal provides evidence for the ability of the dimeric peptide bLFcin(20-25)$_2$ to interact with cell membranes. PE-A: phycoerythrin Signal (for sample A).

including pore formation, irregularities, and vacuolization (Figure 5). As expected, untreated cells remained completely attached to the slide surface and exhibited an extended, homogeneous, and smooth-appearing cytoplasm.

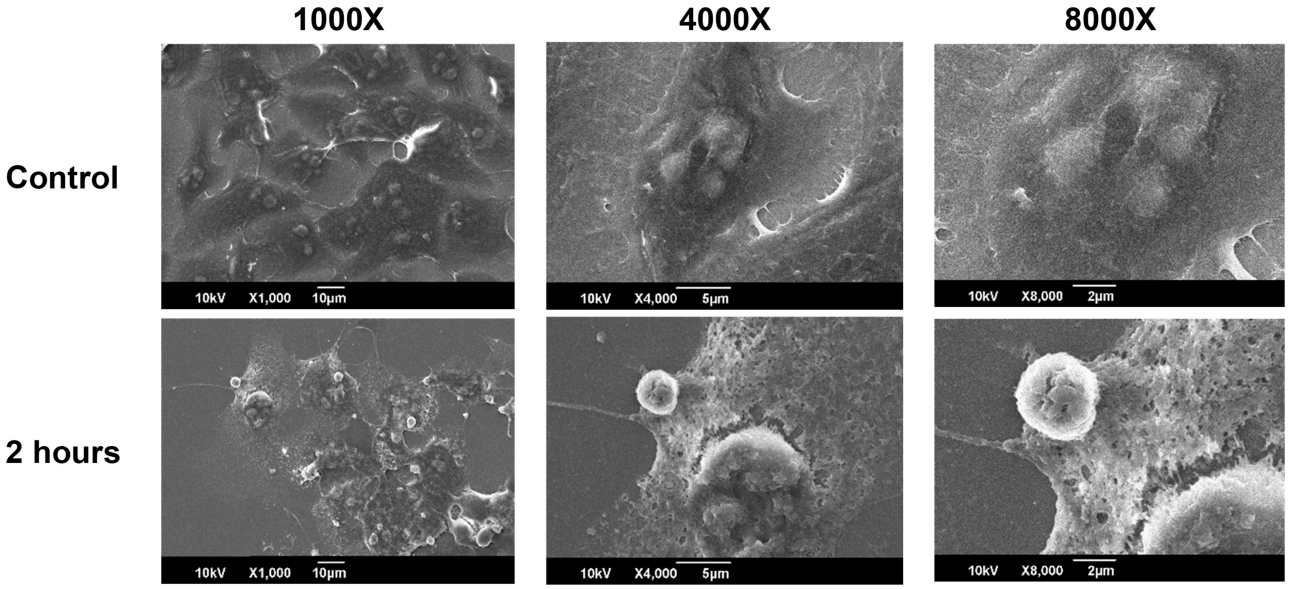

Figure 5. SEM imaging of FaDu cells. The top panel shows control, untreated cells. The bottom panel displays cells treated with 100 µM bLFcin(20-25)$_2$ for 2 h.

Effect of bLFcin(20-25)$_2$ on tumor growth in vivo

While our initial studies in FaDu cells established key features of the dimeric peptide activity in a cellular model of human oral cancer, this is a multistage, tissue- and host-dependent process that cannot be fully modeled in vitro; we employed a previously described methodology to induce oral carcinoma in hamsters [35]. The first animals exhibiting tumors (Group A) served as negative controls and received daily, intratumoral injections of 50 µL saline. Animals in Group B were treated with 100 µM bLFcin(20-25)$_2$ for 15 days (see macroscopic findings in Figure S2). No animals died before the scheduled end of the treatment, and the weight of the animals was registered every week (Figure S3).

Dimer peptide-treated animals developed much smaller tumors compared to the placebo group, as reflected by statistically significant differences in tumor volume (Figure 6). These comparisons were made by assessing volume change ratios, calculated as volume v_n/volume v_0, where v_n was the volume on the day of measurement, and v_0 was the volume on the first day of treatment.

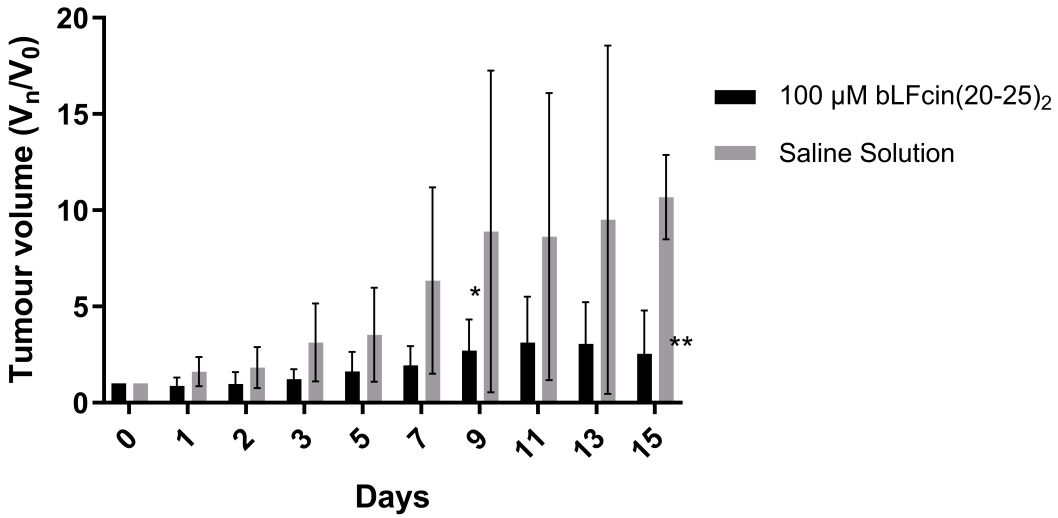

Figure 6. Relative tumor growth (volume Day$_n$/Day$_0$) in mice subjected to the following solutions: saline (closed triangles) and bLFcin(20-25)$_2$ (closed circles).

Microscopic analyses of tissue samples from animals euthanized at the end of each treatment showed the histological features of the carcinoma stage with abundant cell and nuclear pleomorphism and loss of stratification, contrary to the continuous and distinguished epithelial cell layers characteristic of healthy tissue. The microscopic imaging of peptide-treated tumors revealed no signs of cancer lesion regression or significant differences in tissue morphology, compared to the mucosa of saline-treated negative controls. However, the images evidenced substantial lymphocytic cell recruitment to tumors in animals treated with the dimeric peptide dissolved in saline solution (Figure 7). Future studies should investigate the inflammatory markers that characterize the host immune response to peptide administration.

Discussion

A variety of peptides derived from the sequence comprising residues 17–31 of bLFcin(17-31) have been proposed and evaluated as chemotherapeutic candidates. Their cationic charge and amphipathic features seem crucial for specific targeting [26, 44]. Highly active peptides typically have cationic residues, such as Arg, concentrated in one sector, while aromatic residues in the lipophilic sector are critical for maintaining high tumor-killing capability. Previous studies have supported the contribution of Arg and Trp residues to the interaction of these and other bLFcin peptides with bilayer cell membranes; as an example, substituting Ala for either of the Trp residues at positions 6 and 8 in bLFcin(17-31) derivatives results in a significant reduction of antibacterial potency [16]. Following these observations, linear truncated peptides before and after the Arg and Trp-rich motif RRWQWR were evaluated. Our results identify the shortest sequence that retains modest cytotoxic activity. We found that bLFcin(17-30) retained some of the bLFcin activity

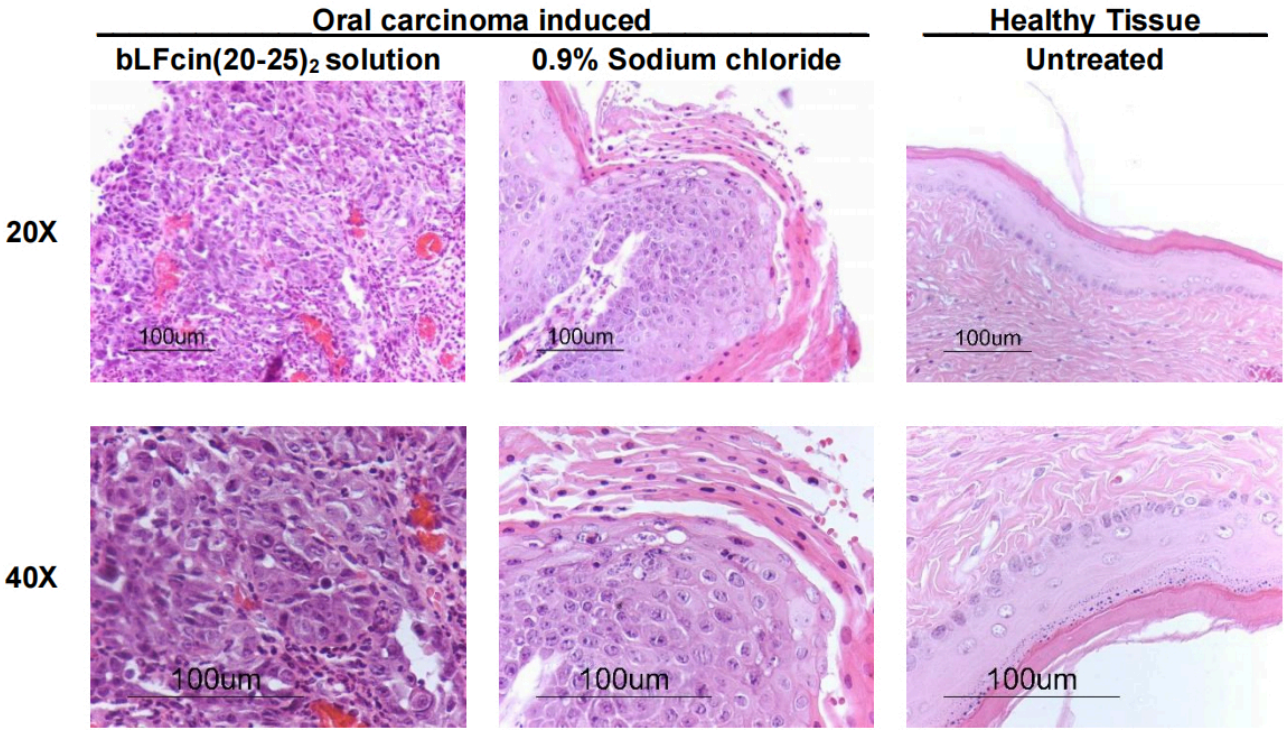

Figure 7. H&E-stained tissue from chemically induced oral cancer tumors in hamsters after 15 days of treatment with bLFcin(20-25)$_2$ and saline (left and central panels) against healthy oral tissue (right panel).

following removal of the alanine C-terminal amino acid. Indeed, treatment of FaDu cells with 100 μM bLFcin(17-30) reduced viability by around 80%, whereas affecting normal HEK001 cells.

In contrast, deletion of the N-terminal phenylalanine residue, whether alone or accompanied by removal of the following amino acids [ranging from bLFcin(18-31) to bLFcin(20-31)], significantly impaired cytotoxic effects. Consequently, the 6-amino acid motif RRWQWR lacked intrinsic cytotoxic activity. This aligns with Richardson et al. [45], who reported that bLFcin(20-25) failed to interact with or disrupt the membranes of Jurkat and CCRF-CEM T-leukemia cells, as well as MDA-MB-231 breast cancer cells. However, they noted it could still interact with mitochondrial membranes and exert cytotoxic potential if delivered intracellularly via fused liposomes. In a different study, the PFR peptide, a 9-amino acid derivative of human lactoferricin (PFWRIRIRR-NH_2), inhibited leukemia cell proliferation by inducing necrosis rather than apoptosis. It acts by disrupting tumor cell membranes and triggering necroptosis through ER stress, elevated calcium levels, and ROS [46]. These findings indicate that cytotoxic activity increases when the cationic charge is enhanced. Our observation that the 6-residue motif and most of the linear peptides lacked cytotoxic activity against SCC adherent cells prompted us to test branched and palindromic sequences. These modified peptides exhibited greater cytotoxicity, likely due to their increased cationic charge: +3 for the linear palindromic motif, +6 for the dimer, and +12 for the tetramer design. The tetrameric peptide bLFcin(20-25)$_4$ was the most cytotoxic agent, reducing FaDu cell viability to nearly zero at 50 μM. Normal keratinocytes had a comparable susceptibility, and SCC9 cancer cells were slightly less sensitive. These observations indicate that the tetrameric peptide lacks selectivity, as it appears toxic to normal cells. Moreover, while the palindromic peptide exhibited greater cytotoxicity than the dimeric sequence in FaDu cells, highlighting its potential as a cytotoxic agent, both bLFcin(20-25)$_4$ and bLFcinPal induced 49.1% and 24.8% hemolysis, respectively [41]. These findings represent important considerations when assessing drug selectivity and safety. Further investigation is needed to better understand the selectivity of both tetrameric and palindromic peptides on SCC cells. Specific evaluation of the z-potential and the negatively charged molecules, like phosphatidylserine or cardiolipin, more highly expressed on the membrane of cancer cells, could give hints on the evaluated peptides' activity.

Since the dimeric peptide was previously reported to have the lowest hemolytic activity and it slightly decreased the viability of FaDu cells by altering their cell membrane structure (Figure 3), bLFcin(20-25)$_2$

was chosen for further characterization. The dimeric branched peptide has a net charge of +6, which enhances its interaction with negatively charged cancer cell membranes [44]. Additionally, its repeated motif, rich in tryptophan and arginine, confers amphipathic properties that facilitate membrane penetration [39]. FC confirmed that bLFcin(20-25)$_2$, but not the linear bLFcin(20-25) peptide, interacted with FaDu cancer cells and normal keratinocytes by over 95%. In addition, the dimeric peptide induced morphological changes, as assessed by electron microscopy. Cell membrane swelling and pore formation induced by cationic peptides have been widely reported; examples include leukemic cell lines treated with the human lactoferricin-derived 'PFR peptide' PFWRIRIRR-NH2 [46], MCF7 breast cancer cells exposed to 50 µg/mL of purified bioactive peptides extracted from *Achillea eriophora* [47], and HT-29 colorectal adenocarcinoma cells treated with non-canonical and D-amino acid modified dimeric bLFcin peptides [42]. While the current study requires further experimentation to fully elucidate the mechanistic and biological markers of cell death induced by the dimeric peptide, we previously observed the necrotic effects of high doses of the tetramer through increased DNA fragmentation via TUNEL reactivity imaging [33]. Consequently, additional analysis is necessary to define whether the cell death pathway triggered by bLFcin(20-25)$_2$ exposure in SCC cells is apoptotic or necrotic.

After observing the cytotoxic potential and cell interactions of bLFcin(20-25)$_2$, we used the dimeric peptide to treat chemically induced oral cancer in hamsters. The DMBA-induced oral carcinoma model is widely accepted for studying oral carcinogenesis, as it mimics tumor development in healthy individuals exposed topically to an anthracene-based carcinogen, simulating tobacco or alcohol use. This disease model progresses through premalignant and malignant stages [48], and it shares key tumor-associated molecular and biophysical features with FaDu cells, including eIF4E overexpression and Akt/mTOR pathway activation, with the subsequent dysregulated apoptotic signaling, such as phosphatidylserine externalization [49]. These conserved characteristics underlie the selective susceptibility of oral SCC cells to cationic, membrane-active peptides, and enable us to conduct complementary studies under physiologically relevant conditions. Following macroscopic detection of cheek tumors, the hamsters were treated intratumorally with a 100 µM solution of dimeric peptide in saline. Peptide-treated tumors grew slightly over the 15-day treatment period, whereas untreated tumors increased 5-fold in volume by day 7. Cationic peptides may target negatively charged tumor cell membranes and induce necrosis. Histological analyses of peptide-treated tissues revealed extensive lymphocytic infiltration and condensed chromatin nuclei, indicative of widespread tumor cell necrosis. Such findings resemble the massive necrotic tissue observed in 4T1 murine breast cancer allografts following a single dose of 1,200 µg of Cypep-1, a 27-amino acid cationic peptide [50]. Similar findings include a reduction in microvessel density observed in xenograft tumors after treatment with Nisin ZP, a *Lactococcus lactis* milk fermentation product [51]. No signs of necrosis were observed in other vital organs (including the brain, heart, lungs, and kidneys), suggesting that the cationic peptide exhibits localized activity when administered intratumorally. Future studies utilizing larger sample sizes, control groups treated with non-active peptides, and marker-specific imaging of excised tissues would provide deeper insights into the peptide's selectivity and its mechanistic mode of action.

We have tested branched derivatives of the 6-amino-acid bLFcin with enhanced cationic and amphiphilic properties to identify sequences that disrupt the membranes of oral cancer cells. This disruption, characterized by membrane leakage and pore formation, was confirmed through electron microscopy. The dimeric branched peptide bLFcin(20-25)$_2$ inhibited tumor growth over a 15-day treatment period. Intratumoral administration of this CAMP induced localized necrosis without affecting vital organs and promoted inflammatory cell recruitment. Further studies are needed to elucidate the underlying mechanism by which bLFcin(20-25)$_2$ induces cytotoxicity and to characterize the nature of potential immunological responses.

Abbreviations

ACN: acetonitrile

bLFcin: bovine lactoferricin

CAMPs: cationic antimicrobial peptides

DCC: dicyclohexylcarbodiimide

DCM: dichloromethane

DMBA: 7,12-dimethylbenz[α]anthracene

DMF: dimethylformamide

EDT: ethane-1,2-dithiol

FC: flow cytometry

Fmoc: 9-fluorenylmethoxycarbonyl

FSC-A: forward scatter (for sample A)

HOBt: 6-HCl 1-hydroxybenzotriazole

HPLC: high-performance liquid chromatography

IC_{50}: half-maximal inhibitory concentration

MALDI–TOF: matrix-assisted laser desorption/ionization–time of flight

OSCC: oral squamous cell carcinoma

PBS: phosphate buffered saline

PE: phycoerythrin

PE-A: phycoerythrin Signal (for sample A)

s.e.m.: standard error of the mean

SAPE: streptavidin-phycoerythrin

SCC: squamous cell carcinoma

SEM: scanning electron microscopy

SPPS: solid-phase peptide synthesis

SSC-A: side scatter (for sample A)

tBu: tert-butyl

TFA: trifluoroacetic acid

TIS: triisopropylsilane

Supplementary materials

The supplementary materials for this article are available at: https://www.explorationpub.com/uploads/Article/file/1008171_sup_1.pdf.

Declarations

Acknowledgments

The authors are grateful to Fundación Ceiba for the PhD scholarship awarded to D.M.

Author contributions

DAMB: Conceptualization, Methodology, Investigation, Formal analysis, Writing—original draft, Visualization, Writing—review & editing. SCVC: Formal analysis, Methodology, Writing—review & editing.

PABG: Conceptualization, Methodology, Resources, Writing—review & editing. JERP: Conceptualization, Methodology, Supervision, Resources, Funding acquisition, Writing—review & editing. All authors read and approved the submitted version.

Conflicts of interest

The authors declare that they have no conflicts of interest.

Ethical approval

All animal experiments complied with the ARRIVE guidelines and the Guide for the Care and Use of Laboratory Animals. They were carried out following the EU directive 2010/63 for the protection of animals used for scientific purposes, and were approved by the Ethics Committee of the Sciences Faculty of the National University of Colombia (approved main project identification: RC# 678 of 2014).

Consent to participate

Not applicable.

Consent to publication

Not applicable.

Availability of data and materials

The raw data supporting the conclusions of this manuscript will be made available by the authors, without undue reservation, to any qualified researcher.

Funding

This study was developed as part of the Project: "Diseño, síntesis química y caracterización de péptidos derivados de lactoferricina y evaluación de su actividad anticancerígena. Fase II" approved by COLCIENCIAS, announcement 657-2014, contract: RC No. [678] of 2014. The funders had no role in study design, data collection and analysis, decision to publish, or preparation of the manuscript.

Publisher's note

Open Exploration maintains a neutral stance on jurisdictional claims in published institutional affiliations and maps. All opinions expressed in this article are the personal views of the author(s) and do not represent the stance of the editorial team or the publisher.

References

1. Gatfield ER, Ince WHJ, Jefferies SJ. Squamous cell carcinoma of the oral cavity, oropharynx and upper oesophagus. Medicine. 2024;52:130–5. [DOI]
2. Pardo C, de Vries E. Oral and oropharyngeal cancer in Colombia: an experience in a middle-income country cancer institute (2004–2013). Oral Cancer. 2018;2:19–26. [DOI]
3. Silvestre-Donat FJ, Puente Sandoval A. Efectos adversos del tratamiento del cáncer oral. Av Odontoestomatol. 2008;24:111–21. [DOI]
4. Yuan J, Shi K, Chen G, Xu W, Qiu L, Fei Y, et al. A Network Meta-Analysis of the Systemic Therapies in Unresectable Head and Neck Squamous Cell Carcinoma. Cancer Control. 2024;31: 10732748241255535. [DOI] [PubMed] [PMC]
5. Chiari F, Filippini DM, Fermi M, Presutti L, Caporale CD, Bertino G, et al. Survival behavior of patients treated with curative and palliative electrochemotherapy for oral and oropharyngeal cancer: a systematic review. Eur Arch Otorhinolaryngol. 2026;283:2665–80. [DOI] [PubMed]

6. Raucher D, Ryu JS. Cell-penetrating peptides: strategies for anticancer treatment. Trends Mol Med. 2015;21:560–70. [DOI] [PubMed]
7. Chu HL, Yip BS, Chen KH, Yu HY, Chih YH, Cheng HT, et al. Novel antimicrobial peptides with high anticancer activity and selectivity. PLoS One. 2015;10:e0126390. [DOI] [PubMed] [PMC]
8. da Costa JP, Carvalhais V, Amado F, Silva A, Nogueira-Ferreira R, Ferreira R, et al. Anti-tumoral activity of human salivary peptides. Peptides. 2015;71:170–8. [DOI] [PubMed]
9. Liu X, Li Y, Li Z, Lan X, Leung P, Li J, et al. Mechanism of Anticancer Effects of Antimicrobial Peptides. J Fiber Bioeng Inform. 2015;8:25–36. [DOI]
10. Xiao YF, Jie MM, Li BS, Hu CJ, Xie R, Tang B, et al. Peptide-Based Treatment: A Promising Cancer Therapy. J Immunol Res. 2014;2015:1–13. [DOI]
11. Wu D, Gao Y, Qi Y, Chen L, Ma Y, Li Y. Peptide-based cancer therapy: opportunity and challenge. Cancer Lett. 2014;351:13–22. [DOI] [PubMed]
12. Morillo I, Zulaica J, R Caballero A, Auzmendi-Iriarte J, Largo E, Apellaniz B, et al. Engineering a single-chain immunoglobulin scaffold loaded with a latent-releasable cytotoxic pore-forming peptide. Commun Biol. 2025;8:1665. [DOI] [PubMed] [PMC]
13. Li C, Li S, Lv L, Chen Y, Yang S, Lu Y, et al. Mitochondria-Targeting Antimicrobial Peptide (AMP) Regulating N6-Methyladenosine (m6A) Modification to Promote Colon Cancer Ferroptosis. Bioconjug Chem. 2025;36:2497–506. [DOI] [PubMed] [PMC]
14. Kapan E, Uslu C, Arab H, Ahmed L, Ali R, Tereshchenkov AG, et al. Toward Mitochondrial Targeting of Resistant Triple-Negative Breast Cancer Using Triphenylphosphonium-Conjugated Antimicrobial Peptides. ACS Pharmacol Transl Sci. 2025;8:4159–71. [DOI] [PubMed] [PMC]
15. Włodarczyk J, Kamysz E, Fichna J. Synthesis and evaluation of KR-12, an LL-37 fragment, and its short-chain fatty acid derivatives: selective cytotoxicity in colorectal cancer cells and anti-tumor efficacy in an azoxymethane/DSS-induced colitis-associated cancer mouse model. Pharmacol Rep. 2025;77:1689–702. [DOI] [PubMed] [PMC]
16. Hao Y, Yang N, Teng D, Wang X, Mao R, Wang J. A review of the design and modification of lactoferricins and their derivatives. Biometals. 2018;31:331–41. [DOI] [PubMed]
17. Vogel HJ, Schibli DJ, Jing W, Lohmeier-Vogel EM, Epand RF, Epand RM. Towards a structure-function analysis of bovine lactoferricin and related tryptophan- and arginine-containing peptides. Biochem Cell Biol. 2002;80:49–63. [DOI] [PubMed]
18. Schibli DJ, Hwang PM, Vogel HJ. The structure of the antimicrobial active center of lactoferricin B bound to sodium dodecyl sulfate micelles. FEBS Lett. 1999;446:213–7. [DOI] [PubMed]
19. Nguyen LT, Schibli DJ, Vogel HJ. Structural studies and model membrane interactions of two peptides derived from bovine lactoferricin. J Pept Sci. 2005;11:379–89. [DOI] [PubMed]
20. Zhang Y, Lima CF, Rodrigues LR. Anticancer effects of lactoferrin: underlying mechanisms and future trends in cancer therapy. Nutr Rev. 2014;72:763–73. [DOI] [PubMed]
21. Yin CM, Wong JH, Xia J, Ng TB. Studies on anticancer activities of lactoferrin and lactoferricin. Curr Protein Pept Sci. 2013;14:492–503. [DOI] [PubMed]
22. Riedl S, Leber R, Rinner B, Schaider H, Lohner K, Zweytick D. Human lactoferricin derived di-peptides deploying loop structures induce apoptosis specifically in cancer cells through targeting membranous phosphatidylserine. Biochim Biophys Acta. 2015;1848:2918–31. [DOI] [PubMed]
23. Wang S, Tu J, Zhou C, Li J, Huang L, Tao L, et al. The effect of Lfcin-B on non-small cell lung cancer H460 cells is mediated by inhibiting VEGF expression and inducing apoptosis. Arch Pharm Res. 2015;38:261–71. [DOI] [PubMed]
24. Sheng M, Zhao Y, Zhang A, Wang L, Zhang G. The effect of LfcinB9 on human ovarian cancer cell SK-OV-3 is mediated by inducing apoptosis. J Pept Sci. 2014;20:803–10. [DOI] [PubMed]
25. Fang B, Zhang M, Tian M, Jiang L, Guo HY, Ren FZ. Bovine lactoferrin binds oleic acid to form an anti-tumor complex similar to HAMLET. Biochim Biophys Acta. 2014;1841:535–43. [DOI] [PubMed]

26. Hilchie AL, Vale R, Zemlak TS, Hoskin DW. Generation of a hematologic malignancy-selective membranolytic peptide from the antimicrobial core (RRWQWR) of bovine lactoferricin. Exp Mol Pathol. 2013;95:192–8. [DOI] [PubMed]
27. Eliassen LT, Haug BE, Berge G, Rekdal O. Enhanced antitumour activity of 15-residue bovine lactoferricin derivatives containing bulky aromatic amino acids and lipophilic N-terminal modifications. J Pept Sci. 2003;9:510–7. [DOI] [PubMed]
28. Mader JS, Richardson A, Salsman J, Top D, de Antueno R, Duncan R, et al. Bovine lactoferricin causes apoptosis in Jurkat T-leukemia cells by sequential permeabilization of the cell membrane and targeting of mitochondria. Exp Cell Res. 2007;313:2634–50. [DOI] [PubMed]
29. Castellar-Almonacid DA, Barragán-Cárdenas AC, Rodríguez-Mejia KG, Maldonado-Sanabria LA, Ardila-Chantré N, Mendoza-Mendoza JD, et al. Non-steroidal anti-inflammatory drugs conjugated to a synthetic peptide exhibit *in vitro* cytotoxic activity against cervical cancer and melanoma cells. RSC Med Chem. 2025;16:4170–82. [DOI] [PubMed] [PMC]
30. León-Calvijo MA, Leal-Castro AL, Almanzar-Reina GA, Rosas-Pérez JE, García-Castañeda JE, Rivera-Monroy ZJ. Antibacterial activity of synthetic peptides derived from lactoferricin against Escherichia coli ATCC 25922 and Enterococcus faecalis ATCC 29212. Biomed Res Int. 2015;2015:453826. [DOI] [PubMed] [PMC]
31. Huertas Méndez NJ, Vargas Casanova Y, Gómez Chimbi AK, Hernández E, Leal Castro AL, Melo Diaz JM, et al. Synthetic Peptides Derived from Bovine Lactoferricin Exhibit Antimicrobial Activity against E. coli ATCC 11775, S. maltophilia ATCC 13636 and S. enteritidis ATCC 13076. Molecules. 2017;22:452. [DOI] [PubMed] [PMC]
32. Vargas Casanova Y, Rodríguez Guerra JA, Umaña Pérez YA, Leal Castro AL, Almanzar Reina G, García Castañeda JE, et al. Antibacterial Synthetic Peptides Derived from Bovine Lactoferricin Exhibit Cytotoxic Effect against MDA-MB-468 and MDA-MB-231 Breast Cancer Cell Lines. Molecules. 2017;22:1641. [DOI] [PubMed] [PMC]
33. Solarte VA, Conget P, Vernot JP, Rosas JE, Rivera ZJ, García JE, et al. A tetrameric peptide derived from bovine lactoferricin as a potential therapeutic tool for oral squamous cell carcinoma: A preclinical model. PLoS One. 2017;12:e0174707. [DOI] [PubMed] [PMC]
34. Vega Chaparro SC, Valencia Salguero JT, Martínez Baquero DA, Rosas Pérez JE. Effect of Polyvalence on the Antibacterial Activity of a Synthetic Peptide Derived from Bovine Lactoferricin against Healthcare-Associated Infectious Pathogens. Biomed Res Int. 2018;2018:5252891. [DOI] [PubMed] [PMC]
35. Martínez B DA, Barato Gómez PA, Iregui Castro CA, Rosas Pérez JE. DMBA-Induced Oral Carcinoma in Syrian Hamster: Increased Carcinogenic Effect by Dexamethasone Coexposition. Biomed Res Int. 2020;2020:1470868. [DOI] [PubMed] [PMC]
36. Vergel Galeano CF, Rivera Monroy ZJ, Rosas Pérez JE, García Castañeda JE. Efficient Synthesis of Peptides with 4-Methylpiperidine as Fmoc Removal Reagent by Solid Phase Synthesis. J Mex Chem Soc. 2014;58:386–92. [DOI]
37. Faustino-Rocha A, Oliveira PA, Pinho-Oliveira J, Teixeira-Guedes C, Soares-Maia R, da Costa RG, et al. Estimation of rat mammary tumor volume using caliper and ultrasonography measurements. Lab Anim (NY). 2013;42:217–24. [DOI] [PubMed]
38. Mader JS, Salsman J, Conrad DM, Hoskin DW. Bovine lactoferricin selectively induces apoptosis in human leukemia and carcinoma cell lines. Mol Cancer Ther. 2005;4:612–24. [DOI] [PubMed]
39. Eloïse L, Petit L, Nominé Y, Heurtault B, Ben Hadj Kaddour I, Senger B, et al. The antibacterial properties of branched peptides based on poly(l-arginine): In vitro antibacterial evaluation and molecular dynamic simulations. Eur J Med Chem. 2024;268:116224. [DOI] [PubMed]
40. Solarte VA, Rosas JE, Rivera ZJ, Arango-Rodríguez ML, García JE, Vernot JP. A Tetrameric Peptide Derived from Bovine Lactoferricin Exhibits Specific Cytotoxic Effects against Oral Squamous-Cell Carcinoma Cell Lines. Biomed Res Int. 2015;2015:630179. [DOI] [PubMed] [PMC]

41. Vega SC, Martínez DA, Chalá MDS, Vargas HA, Rosas JE. Design, Synthesis and Evaluation of Branched RRWQWR-Based Peptides as Antibacterial Agents Against Clinically Relevant Gram-Positive and Gram-Negative Pathogens. Front Microbiol. 2018;9:329. [DOI] [PubMed] [PMC]
42. Cárdenas-Martínez KJ, Reyes-Calderon JE, Parra-Giraldo CM, Vargas-Casanova Y, Barragán-Cárdenas AC, Fierro-Medina R, et al. Behind anticancer molecules: lactoferricin dimeric peptides with fast, selective, persistent and broad-spectrum cytotoxic effect. Explor Drug Sci. 2025;3:100891. [DOI]
43. Huni KC, Cheung J, Sullivan M, Robison WT, Howard KM, Kingsley K. Chemotherapeutic Drug Resistance Associated with Differential miRNA Expression of miR-375 and miR-27 among Oral Cancer Cell Lines. Int J Mol Sci. 2023;24:1244. [DOI] [PubMed] [PMC]
44. Strøm MB, Haug BE, Rekdal O, Skar ML, Stensen W, Svendsen JS. Important structural features of 15-residue lactoferricin derivatives and methods for improvement of antimicrobial activity. Biochem Cell Biol. 2002;80:65–74. [DOI] [PubMed]
45. Richardson A, de Antueno R, Duncan R, Hoskin DW. Intracellular delivery of bovine lactoferricin's antimicrobial core (RRWQWR) kills T-leukemia cells. Biochem Biophys Res Commun. 2009;388: 736–41. [DOI] [PubMed]
46. Lu Y, Zhang TF, Shi Y, Zhou HW, Chen Q, Wei BY, et al. PFR peptide, one of the antimicrobial peptides identified from the derivatives of lactoferrin, induces necrosis in leukemia cells. Sci Rep. 2016;6: 20823. [DOI] [PubMed] [PMC]
47. Taghizadeh MS, Niazi A, Moghadam A, Afsharifar AR. Novel bioactive peptides of Achillea eriophora show anticancer and antioxidant activities. Bioorg Chem. 2021;110:104777. [DOI] [PubMed]
48. Chen YK, Lin LM. DMBA-induced hamster buccal pouch carcinoma and VX2-induced rabbit cancer as a model for human oral carcinogenesis. Expert Rev Anticancer Ther. 2010;10:1485–96. [DOI] [PubMed]
49. Stadler ME, Patel MR, Couch ME, Hayes DN. Molecular biology of head and neck cancer: risks and pathways. Hematol Oncol Clin North Am. 2008;22:1099–124. [DOI] [PubMed] [PMC]
50. Szczepanski C, Tenstad O, Baumann A, Martinez A, Myklebust R, Bjerkvig R, et al. Identification of a novel lytic peptide for the treatment of solid tumours. Genes Cancer. 2014;5:186–200. [DOI] [PubMed] [PMC]
51. Kamarajan P, Hayami T, Matte B, Liu Y, Danciu T, Ramamoorthy A, et al. Nisin ZP, a Bacteriocin and Food Preservative, Inhibits Head and Neck Cancer Tumorigenesis and Prolongs Survival. PLoS One. 2015;10:e0131008. [DOI] [PubMed] [PMC]